

Article

Evaluating the Effects of Different Improvement Strategies for the Outdoor Thermal Environment at a University Campus in the Summer: A Case Study in Northern China

Lina Yang¹, Jiying Liu^{2,*}  and Shengwei Zhu^{3,*} ¹ Department of Civil Engineering, Shandong Xiandai University, Jinan 250104, China² School of Thermal Engineering, Shandong Jianzhu University, Jinan 250101, China³ Department of Mechanical Engineering, University of Maryland, College Park, MD 20742, USA

* Correspondence: jxl83@sdjzu.edu.cn (J.L.); szhu918@umd.edu (S.Z.)

Abstract: A lack of consideration of outdoor spaces of universities has resulted in lower outdoor thermal comfort in summer. This study investigates the thermal comfort of outdoor spaces of a university in summer and proposes the model's accuracy and optimization strategies to improve the outdoor thermal environment, including vegetation greening, building morphology, and surface albedo. The ENVI-met program was used for the simulation. The measured data were utilized to verify the accuracy of the simulation model. The typical meteorological year data were applied as the inlet boundary condition of the optimized case. The simulation results show that vegetation greening has the most significant effect on improving the outdoor thermal environment. At a greening rate of 45%, the air temperature (T_a), mean radiant temperature (T_{mrt}), and physiological equivalent temperature (PET) in the study area were 3.2 °C, 14.4 °C, and 6.9 °C lower, respectively, than that in the base case. In areas shaded by building, the T_a , T_{mrt} , and PET were 2 °C, 8.7 °C, and 5.5 °C lower, respectively, than that in the base case. Increasing the height of buildings did not significantly improve thermal comfort when the height-to-width ratio (H/W) exceeded 1.0. Increasing the ground albedo from 0.2 (base case) to 0.6 can reduce the T_a by 1.44 °C but increase the T_{mrt} by 3.7 °C and the PET by 4.3 °C. These findings can be used by urban planners to develop sustainable cities and improve thermal comfort on university campuses.

Keywords: outdoor thermal environment; thermal comfort; improvement strategies; campus planning; university campus



Citation: Yang, L.; Liu, J.; Zhu, S. Evaluating the Effects of Different Improvement Strategies for the Outdoor Thermal Environment at a University Campus in the Summer: A Case Study in Northern China. *Buildings* **2022**, *12*, 2254. <https://doi.org/10.3390/buildings12122254>

Academic Editors: Bo Hong, Yang Geng and Dayi Lai

Received: 23 November 2022

Accepted: 14 December 2022

Published: 17 December 2022

Publisher's Note: MDPI stays neutral with regard to jurisdictional claims in published maps and institutional affiliations.



Copyright: © 2022 by the authors. Licensee MDPI, Basel, Switzerland. This article is an open access article distributed under the terms and conditions of the Creative Commons Attribution (CC BY) license (<https://creativecommons.org/licenses/by/4.0/>).

1. Introduction

The outdoor thermal environment affects people using outdoor spaces, especially on university campuses [1–3]. Campuses have a high density of people performing various activities [4,5]; thus, outdoor thermal comfort affects the daily activities of teachers and students [6–8]. The number of newly-built and expanded campuses has increased recently, but the lack of outdoor space planning has caused students to experience high thermal stress in summer [9–12]. The extensive use of concrete and asphalt in newly-built campuses has increased the surface temperature. A reduction in the proportion of green areas and permeable surfaces has reduced the shading level and heat dissipation rate in summer. The surface materials of buildings absorb heat, but the shading by buildings has not been sufficiently utilized. Moreover, the heat produced by people and heat dissipation equipment has contributed led to low outdoor thermal comfort [13,14]. In other words, in the context of global warming, higher summer temperatures and a lack of planning for campus construction affect students' physical and mental health [15,16].

Various indices have been used to evaluate outdoor thermal comfort on the campus and other urban open spaces [17–19]. For instance, Altunkasa and Uslu [20] analyzed the predicted mean vote (PMV) to reveal the effect of different planting design on thermal

comfort of the campus environment. They concluded that deciduous trees had a larger effect on thermal comfort. The physiological equivalent temperature (PET) and universal thermal climate index (UTCI) are commonly used to determine the neutral temperature in the climate regions they studied [21–23]. Kumar [24] found that the PET was adopted more frequently than other parameters for analyzing outdoor thermal comfort. These studies have demonstrated the usefulness of these models for designing outdoor spaces, however the applicability of these models differs for different cases. PMV [25] is more suitable for evaluating indoor thermal environments. Nie [26] suggested that the UTCI should not be used in cold and severely cold regions in winter.

Methods to mitigate thermal stress in summer include changing the urban geometry, increasing vegetation cover, changing the surface material albedo, and adding water bodies [9,27,28]. Greening is considered a suitable strategy for improving the outdoor thermal environment [29,30]. It reduces the air temperature by shading, reflecting, and absorbing solar radiation and by photosynthesis and transpiration. Numerous researchers have conducted studies on the greening rate, planting configuration, and tree species [31–33]. Wang and Akbari [34] found that a 10% increase in urban vegetation cover reduced the mean radiant temperature (T_{mrt}) by up to 8.3 K. Abdi et al. [35] found that a rectangular planting pattern, the combination of evergreen and deciduous trees, and plantings perpendicular to the prevailing wind direction were the most beneficial to improving the outdoor thermal environment on campus. Gachkar et al. [36] concluded that trees with tall trunks in summer and a high albedo in winter were the best planting strategies in Iran. Yang et al. [37] found that tall trees were more beneficial to improving the outdoor thermal environment than shrubs and grass.

The influence of urban morphological parameters on the outdoor thermal environment cannot be ignored [38,39]. The architectural layout, height, orientation, density, floor area ratio, height-to-width ratio (H/W), and sky view factor (SVF) are the dominant factors affecting radiative and convective heat exchange in urban spaces [40–42]. The H/W is an important parameter describing the openness of streets. Streets with a high H/W can block solar radiation and tend to have higher thermal comfort in summer [43–45]. The SVF is often used to describe the openness of complex outdoor spaces. A lower SVF indicates lower solar radiation [46]. However, a large H/W affected the sunlight hours, especially in cold and severe cold climate zones [47].

Choosing surfaces with a high albedo is an effective strategy for reducing surface temperatures [48,49]. These surfaces absorb less solar energy and have a lower convective heat transfer from the surface to the air [50,51], resulting in lower air temperatures than in areas with low-albedo surfaces [52]. High-albedo surfaces have been used on the ground and on the building envelope and roof (e.g., grassy areas and light-colored stone) [53–55]. However, several researchers have observed an increase in the total radiation due to an increase in reflected shortwave radiation [56]. For example, Yang [57] found that a high-albedo surface increased the thermal stress of pedestrians.

A reasonable optimization strategy is essential to improve the outdoor thermal comfort of teachers and students on campuses. Most studies have focused on urban greening, building layout and structure, and surface albedo and investigated improvements in the outdoor thermal environment in summer using a single factor, whereas few researchers considered multiple factors. This study evaluates the outdoor thermal environment of open space on a university campus considering various design factors and proposes suitable optimization strategies. An ENVI-met program simulation and parameter analysis are used to determine the design requirements of the outdoor thermal environment on the campus in summer to provide theoretical and design information for campus planning.

2. Methods

2.1. Study Area and Climatic Conditions

The research site is located in Jinan City, Shandong Province. The study area is a building on the campus of Shandong Jianzhu University and its surroundings, as shown in

Figure 1. Jinan is a cold region that is hot and rainy in summer and cold and dry in winter. According to the meteorological data from the recent thirty years, Jinan has the highest temperatures in June and August, with average daily maximum temperatures between 31 °C and 33 °C. The maximum temperature is 39 °C. July and August have the largest rainfall and are the months with high temperatures and high humidity (Figure 2). The solar radiation is intense during this period, causing the students to feel uncomfortable in the outdoor environment.



Figure 1. Satellite image of the study area.

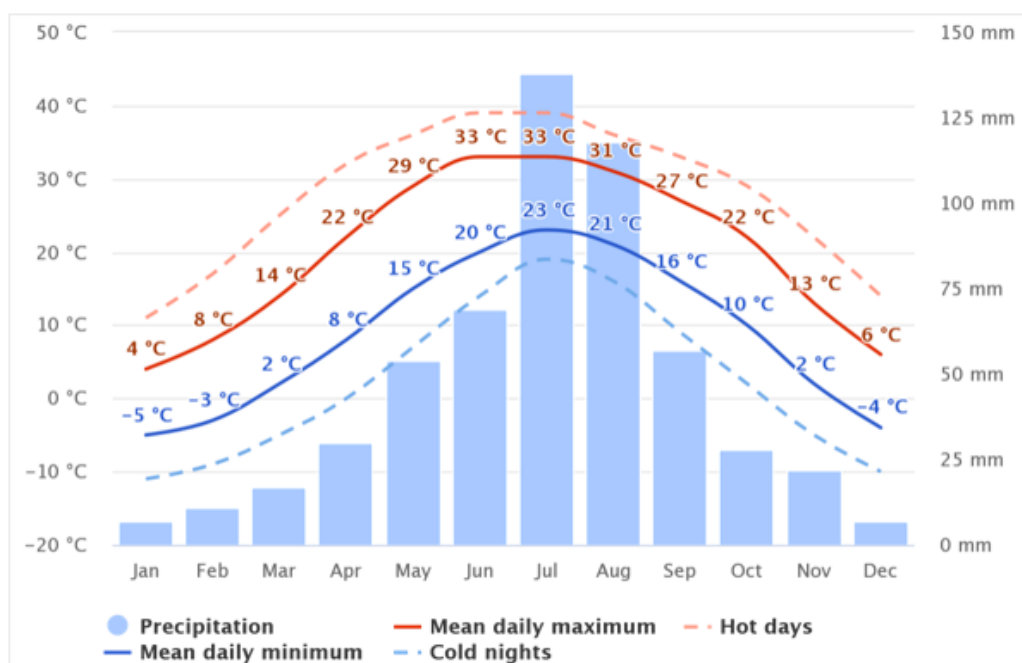


Figure 2. The monthly mean climatic data for Jinan city during a 30-year period obtained from Meteoblue (2022) [58].

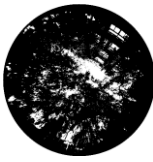
2.2. Field Measurements

The study was conducted from 17 to 18 August 2020 on the two hottest days of the year. Eight measuring points were selected based on the diversity of the thermal environment in the public space. The measurement points are shown in Figure 3, and the site photos and fisheye images of the measurement points are shown in Table 1.



Figure 3. The location of measurement points in the target building and the surrounding area.

Table 1. Surrounding environment of eight measurement points.

Measurement Point	Site Environment	Fisheye Photos	SVF	Measurement Point	Site Environment	Fisheye Photos	SVF
Point 1			0.799	Point 2			0.526
Point 3			0.157	Point 4			0.531
Point 5			0.531	Point 6			0.728
Point 7			0.778	Point 8			0.855

Eight measurement points were selected through field survey based on variation in landscape element and azimuth. The measurement points 1, 2, 3, and 4 were located in the square of the building, and the measurements were obtained at a height of 1.5 m. Points

1 and 2 were located near the building on the north side. There were no tall trees and relatively little shade all day. Point 4 was located in the center of the U-shaped square, which has little shade. The air temperature and relative humidity were measured using an iButton thermometer shielded from the sun by light louvers, and the wind speed and globe temperature were recorded using a JA-IAQ-50 multifunction tester. The solar radiation was measured with a HOBO solar radiation sensor attached to a tripod. An infrared thermometer was used to record hourly thermal images manually, and the fisheye images of the sites were acquired with a fisheye camera. The measurements were obtained at four azimuth angles at a height of 4 m. An L99-FSFX anemometer was used to record the wind speed and direction at the four measuring points. Except for the surface temperature of building envelope and ground, which was measured and recorded manually by the infrared thermometer with an interval of 60 min, other thermal environment parameters were recorded automatically with an interval of 1 min. The details of the devices are listed in Table 2.

Table 2. The measurement parameters and devices used for monitoring.

Instrument	Parameters	Accuracy	Measuring Range
iButton thermometer	Temperature	± 0.5 °C	$-10\sim 65$ °C
iButton thermometer	Humidity	± 0.5 %	0~100%
JA-IAQ-50 multifunction tester	Wind speed	± 0.03 m/s	0~2 m/s
JA-IAQ-50 multifunction tester	Globe temperature	± 0.5 °C	$-20\sim 120$ °C
L99-FSFX anemometer	Wind speed	$\pm(0.5 + 0.05 \times \text{speed})$ m/s	0~60 m/s
L99-FSFX anemometer	Wind direction	0~360°	1°
HOBO solar radiation sensor	Solar radiation	± 10 W/m ²	0~1280 W/m ²
Fotric 225s-L24 camera	Surface temperature	± 2 °C	$-20\sim 350$ °C
Fish-eye camera	Fisheye images	-	180°

2.3. Thermal Comfort Indices

In this study, the T_{mrt} and PET were used as indices to evaluate outdoor thermal comfort. The T_{mrt} is the most critical parameter in biological meteorology and outdoor thermal comfort studies. It is defined as the temperature of an ideal isothermal enclosure in which the radiant heat transfer from a human body is equal to the heat transfer in a non-isothermal enclosure. It is calculated as follows [59,60].

$$T_{mrt} = \left[(T_g + 273.15)^4 + \frac{1.10 \times 10^8 V_a^{0.6}}{\epsilon D^{0.4}} \right]^{\frac{1}{4}} - 273.15, \quad (1)$$

where T_g is the black globe temperature (°C), T_a is the air temperature (°C), V_a is the wind speed (m/s), ϵ is the emissivity ($\epsilon = 0.95$ for a black globe), and D is the globe diameter ($D = 50$ mm in this study).

The PET was proposed by Hoppe and is based on the Munich Energy-balance Model for Individuals (MEMI). It is defined as the temperature of an environment resulting in the same physiological response of a subject as in the environment being investigated. It is equal to the core temperature and skin temperature of a person in a standard space (air temperature is 20 °C, relative humidity is 50%, and airflow speed is 0.1 m/s). It takes into account meteorological parameters (including air temperature, relative humidity, wind speed, and solar radiation) and personal data (including height, weight, age, clothing, and activity), so the given thermal feeling is true and reliable. In this study, Biomet, a subroutine of ENVI-met, is used to calculate the PET. The Biomet calculation is based on the RayMan model [2,61–63].

2.4. Simulation Methodology

2.4.1. Simulation Model

ENVI-met is a microclimate simulation software based on fluid mechanics, thermodynamics, and urban ecology. It considers the interaction of surfaces, vegetation, buildings, and the atmosphere in urban environments in simulating dynamic changes in the urban atmosphere. It includes airflow, turbulence, heat and water exchange between plants and the surrounding environment, particle diffusion, and heat and water vapor exchanges between the ground and building surface. ENVI-met has been used extensively for analyzing urban configurations, street canyons, surface materials, greening of buildings and roofs, and wall materials [56,64–68]. Its reliability in simulating urban outdoor thermal environments has been confirmed [20,35].

2.4.2. ENVI-Met Simulation Setting

The simulated area is the chosen building on the university campus and its surroundings. A UAV was used to acquire images of the research area, and an orthophoto mosaic was created as the base map of the ENVI-met model. The image was transformed into the BMP format and imported into the submodule SPACES. The buildings, plants, and grounds in the study area were simulated according to actual conditions (Figure 4). The model was verified using the parameter values in Table 3. The parameter settings included the grid settings, start and end time of the simulation, output time interval of the results, and meteorological conditions. Measurements were used to set the meteorological boundary conditions (including air temperature, relative humidity, and solar radiation). ENVI-met cannot simulate the wind field over time. Therefore, we used the average wind speed during the test days (1.5 m/s at a height of 10 m). Equation (2) was used to determine it, and the most frequent wind direction was 225°.

$$V_{a10} = V_{a0} \left(\frac{z_{10}}{z_0} \right)^\alpha \quad (2)$$

where V_{a10} is the wind speed at 10 m above the ground, and V_{a0} is the wind speed at 1.5 m above the test height. Z_{10} is the distance from the ground (10 m), and z_0 is the height of the anemometer (1.5 m); α is 0.36.

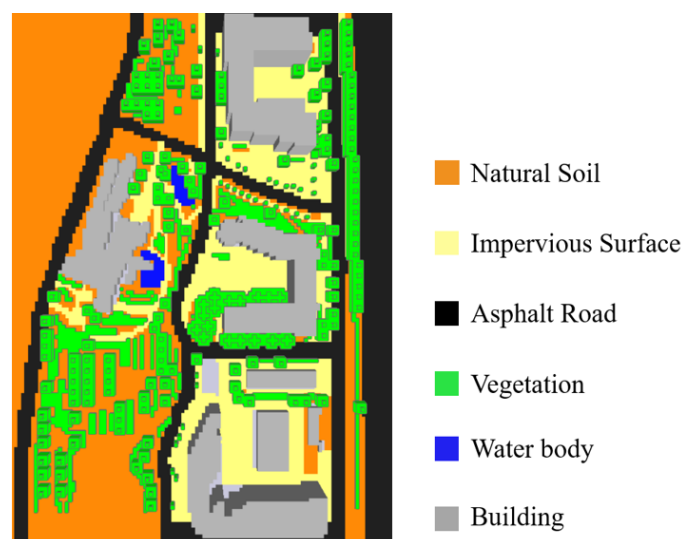


Figure 4. Top view of the simulated area for the actual conditions.

Table 3. Simulation conditions used in ENVI-met.

Variable	Value
Longitude, Latitude	117°14' E, 36°37' N
Climate type	Cold climate
Simulation date	17 August 2020
Simulation duration	48 h
Start time	00:00 am
Spatial resolution	3 × 3 × 3 m ³
Domain Size	336 × 486 × 90 m ³
Model rotation	14°
Wind speed at 10 m	1.5 m/s
Wind direction	225°
Surface albedo	Walls 0.2; Roofs 0.2 and 0.3

Different cases were used to compare the effects of the greening rate, building H/W, and surface albedo on the outdoor thermal environment. Figure 4 shows the top view geometry model as the base case A0. This base case has a greening rate of 12%, a masonry floor albedo of 0.3, and an asphalt floor albedo of 0.2. Besides it, there are additional 13 cases considering the different greening rates, building H/W, and surface albedo. Tables 4–6 are the descriptions of 13 cases under three different optimization strategies, respectively. We used typical meteorological year data in summer as the boundary condition of the model. The other settings were the same as those of the validation model. Three greening rates were considered with a ratio of trees to grassland of 1:1: A1 (25%), A2 (35%), and A3 (45%). The study area is relatively open and consists of mostly low-rise teaching buildings. We simulated additional buildings with different H/W, SVFs, and building heights. As shown in Figure 5, buildings 1, 2, 3, and 4 are the new buildings. According to the principle of using a symmetrical H/W and a suitable floor area ratio proposed by Oke [69] in 1988 and Ali-Touder et al. [64] in 2006, three cases were considered (A4, A5, and A6). The width difference between the new buildings and the original building was 30 m. The new buildings exceeded the height limit of 4–6 floors and had heights of 24 m, 36 m, and 48 m. The albedo of the asphalt was increased from 0.2 (base case) to 0.3, 0.4, 0.5, and 0.6, and the cases were A7, A8, A9, and A10, respectively. The albedo of the masonry floor was increased from 0.3 (base case) to 0.4, 0.5, and 0.6, and the cases were A11, A12, and A13, respectively.

Table 4. Cases for vegetation greening.

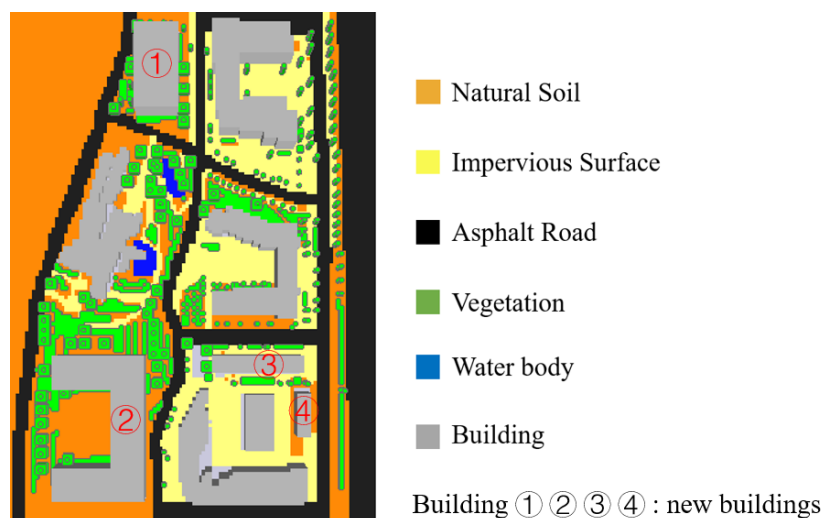
Cases	Greening Rate
A1	25%
A2	35%
A3	45%

Table 5. Cases for building layout.

Cases	H/W	SVF	Building Height
A4	0.8	0.53	24
A5	1	0.457	36
A6	1.2	0.414	48

Table 6. Cases for ground albedo.

Cases	Masonry Floor Albedo	Asphalt Floor Albedo
A7	0.3	0.3
A8	0.3	0.4
A9	0.3	0.5
A10	0.3	0.6
A11	0.4	0.2
A12	0.5	0.2
A13	0.6	0.2

**Figure 5.** Top view of optimized model of building layout.

3. Results

3.1. Measured Results and Simulation Verification

3.1.1. Measurement of Environmental Parameters

We analyzed the climatic characteristics of four measuring points in the building square. Since the wind speed did not change substantially, we only analyzed the changes in the mean temperature and solar radiation at hourly intervals over two days (Figure 6). The daytime temperature was relatively high. The temperature at measuring points one, two, and four were above 36 °C from 10:00 to 16:00, resulting in the discomfort of students during outdoor activities. The temperature reached its peak at 15:00. The maximum temperature was observed at point one (38.4 °C). This point is located on the south side of the building, and there is no shade, and the largest SVF value was recorded (0.799). Point three had the smallest SVF value (0.157) because of vegetation and building shading, where the lowest temperature was observed. The temperature at point three was 0.7–4.1 °C lower than at point one. The solar radiation changed substantially during the day, rapidly increasing from 9:00 h, reaching the peak ($G = 802 \text{ W/m}^2$) at 13:00. Unlike the air temperature, the solar radiation declined after 13:00, which was related to the long-wave radiation of buildings and the ground.

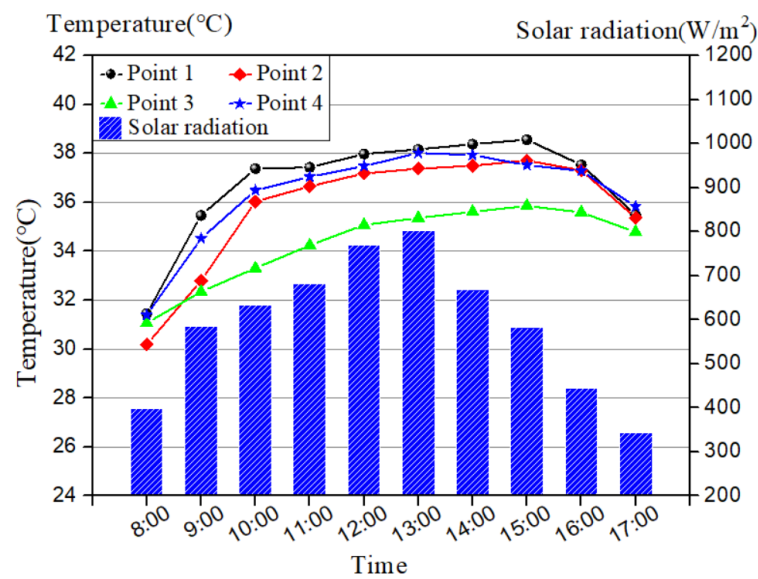


Figure 6. Air temperature and solar radiation at measuring points.

Thermal images are useful in analyzing differences in the surface temperature of different materials. Figure 7 shows thermal images from different locations inside the outdoor open space obtained at 12 h noon. The surface temperatures differed substantially for different materials and at different positions. The windows and walls had high surface temperatures, ranging from 44 °C to 51 °C. The temperature of the ground reached 47.1 °C, far higher than the ambient air temperature. Because of the low albedo, the surface temperature of green plants was about 35 °C. The lowest surface temperature was observed on a wall shaded by buildings and vegetation (31.6 °C). Therefore, shading and a high-albedo surface can substantially reduce the surface temperature and improve students' thermal comfort.

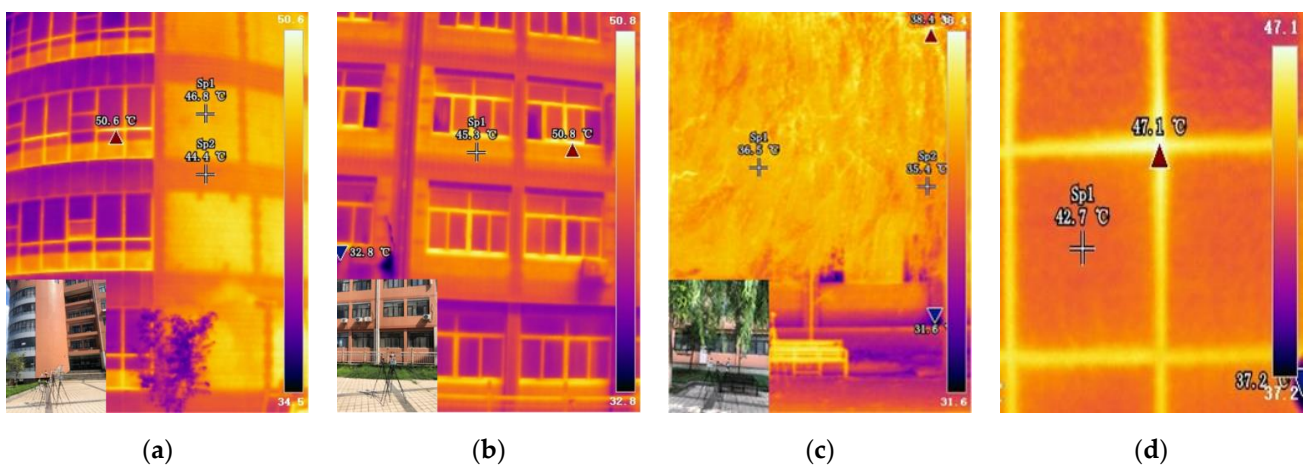


Figure 7. Results of the thermography carried out at 12:00. (a) Point 1; (b) Point 2; (c) Point 3; (d) ground.

3.1.2. ENVI-Met Model Validation

Measuring points two and four are representative measuring points to verify the accuracy of the ENVI-met model. Figure 8 shows the difference between the measured and simulated average meteorological parameters at different points. A good agreement is observed between the measured and simulated air temperature and relative humidity, with a similar trend. This is to note that the curves of the simulation results are flatter than that of the measured results. At the same time, the correlation level between measured

meteorological parameters and simulation results was compared. As shown in Figure 9, the R^2 values between the simulation and measurement results were above 0.9 for points two and four. These comparisons demonstrate the accuracy of the simulation output.

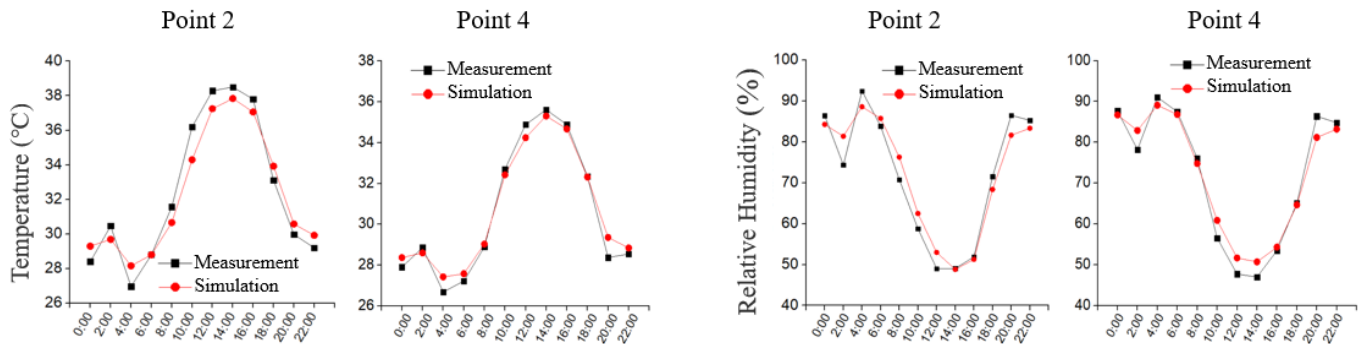


Figure 8. Comparison of measurement and ENVI-met simulation results at points 2 and 4.

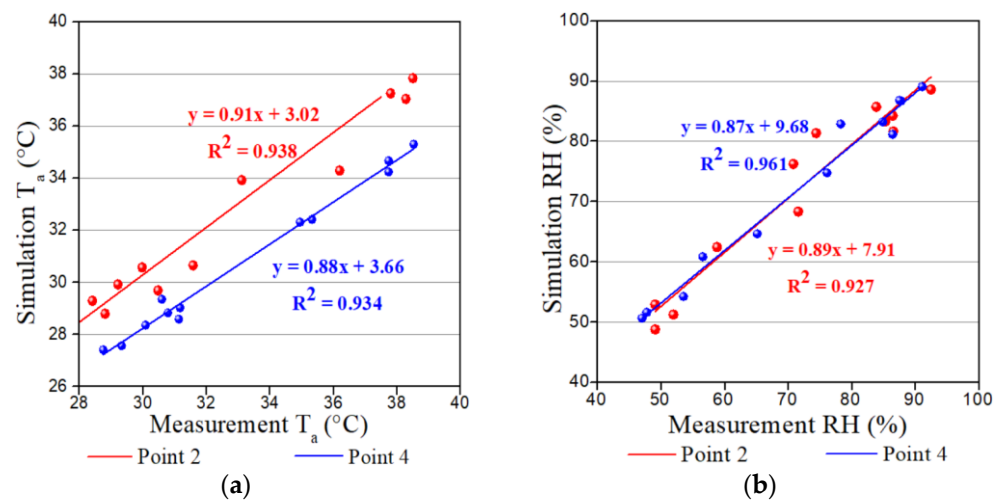


Figure 9. Regression results between measured and simulated values of (a) temperature and (b) relative humidity.

3.2. Effect of Greening Rate

The simulation results showed that the highest temperature occurred at 15:00. The temperature ranged from 34.4 to 37.6 °C, indicating uncomfortable conditions for students in the outdoor environment. Figure 10 shows the air temperature at 15:00 at the pedestrian height of 1.5 m for greening rates of 25%, 35%, and 45% (the legend applies to all cases). It is observed that the air temperature is lower in vegetated than in non-vegetated areas. As the greening rate increases, the temperature decreases. The maximum temperature difference between the area with a 45% greening rate and the base case is 3.2 °C.

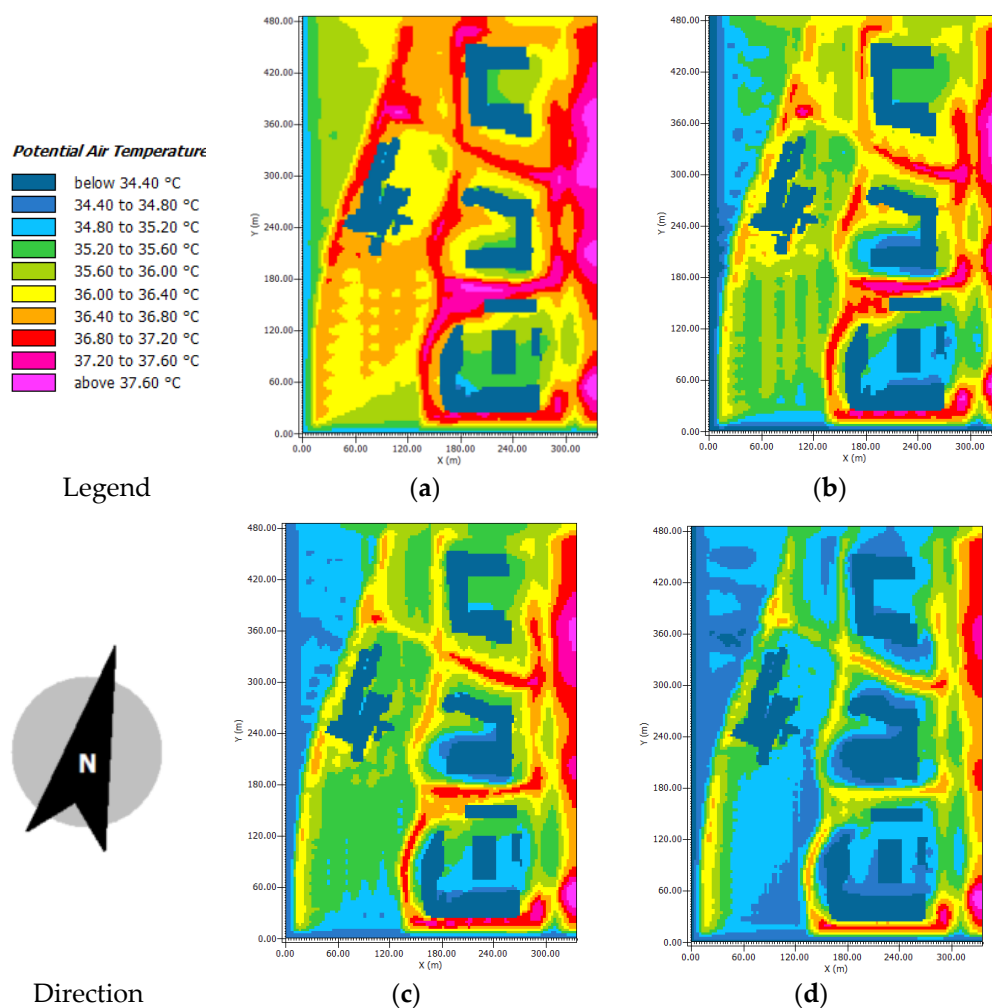


Figure 10. Comparison of simulated T_a obtained at the height of 1.5 m at 15:00 for different greening rates. (a) Base case (A0); (b) Greening rate: 25% (A1); (c) Greening rate: 35% (A2); (d) Greening rate: 35% (A3).

The results show that a dense green space around the campus helps to reduce the air temperature of the environment. These areas include tree plantings and the surrounding square. The statistics show that more than 90% of the temperature values of the A3 case are between 34.4 °C and 36 °C, whereas the percentage is less than 20% for A0. The temperature in areas shaded by buildings is 0.4–1.6 °C lower than that in the common green area. Due to building shade, the air temperature is much lower on the north side of the building than on the south side at the same planting density. Therefore, planting tall trees on the south side of buildings can improve the outdoor thermal environment.

Figure 11 shows the average T_{mrt} at the measuring points at the pedestrian height of 1.5 m for the base case and cases with different greening rates. A0 has a very high T_{mrt} , exceeding 60 °C at 12:00 and 13:00, resulting in extreme discomfort to the human body. Differences in the T_{mrt} are observed between the cases with different greening rates during the day. A small difference occurs at 8:00 (ranging from 0.98 °C to 2 °C). The difference increases over time. For example, the T_{mrt} difference between A0 and A3 is 14.4 °C at 12:00. Therefore, increasing the greening rate can substantially reduce the T_{mrt} , especially at noon, improving outdoor human comfort.

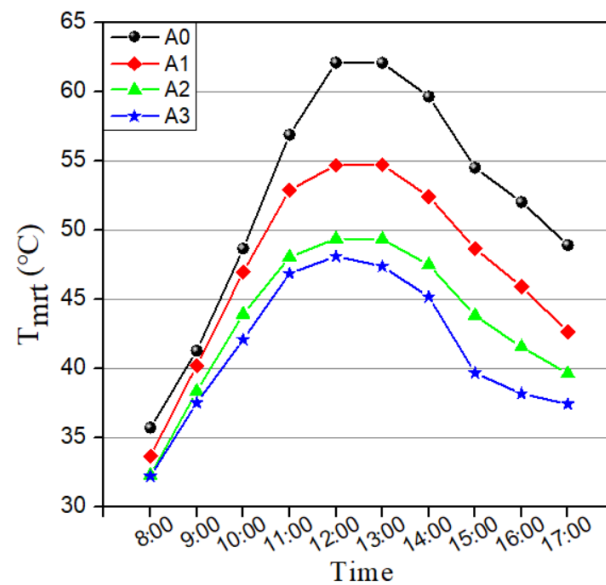


Figure 11. T_{mrt} of the base case and cases with different greening rates.

The PETs are compared at the start of the day (8:00), at noon (12:00), and when the temperature starts to drop (15:00) (Figure 12). The PETs are significantly lower at higher greening rates, reducing thermal discomfort. Compared with the A0 case, a small difference occurs between the cases at 8:00 (0.1–1.3 °C) and a large difference at 12:00 (1.6–5.8 °C). The largest difference is observed at 15:00 (1.2 °C to 6.7 °C). A3, with the highest greening rate (45%), has the lowest PET. It is 5.5 °C lower than that of A1 with the 25% greening rate. These results demonstrate that increasing the greening rate can considerably improve outdoor thermal comfort.

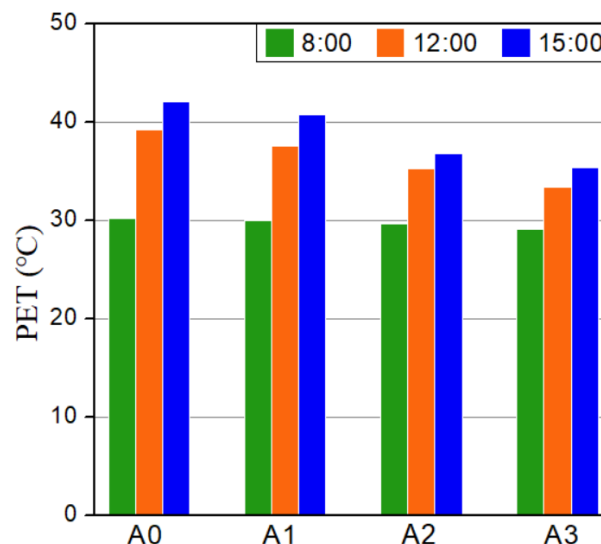


Figure 12. PET of the base case and cases with different greening rates at 8:00, 12:00, and 15:00.

3.3. Effect of Building H/W

The influence of the building H/W on the outdoor thermal environment is evaluated by increasing the building height. Figure 13 shows the air temperature at 15:00 at the pedestrian height for different H/W. The simulation shows that the ranking of the cases based on the average temperature is A0 > A4 > A5 > A6. The proportion of air temperature values above 36.8 °C is 3% for A6 and 13.5% for A0. The temperature around the building is significantly lower due to the shading of the building. As the H/W increases, the air temperature in the study area decreases. The reason is that increasing the building height

reduces the SVF, causing more shading. A larger shadow area means less solar radiation, lowering the temperature of the study area. The proportion of temperature values above 36 °C decreases significantly with an increase in the H/W, especially around buildings, and the temperatures are 0.8 °C to 2 °C cooler for cases A4 than case A0. However, there is a negligible difference in the temperature between A5 and A6, indicating that when the building reaches a certain height, the cooling effect decreases, which is related to SVF.

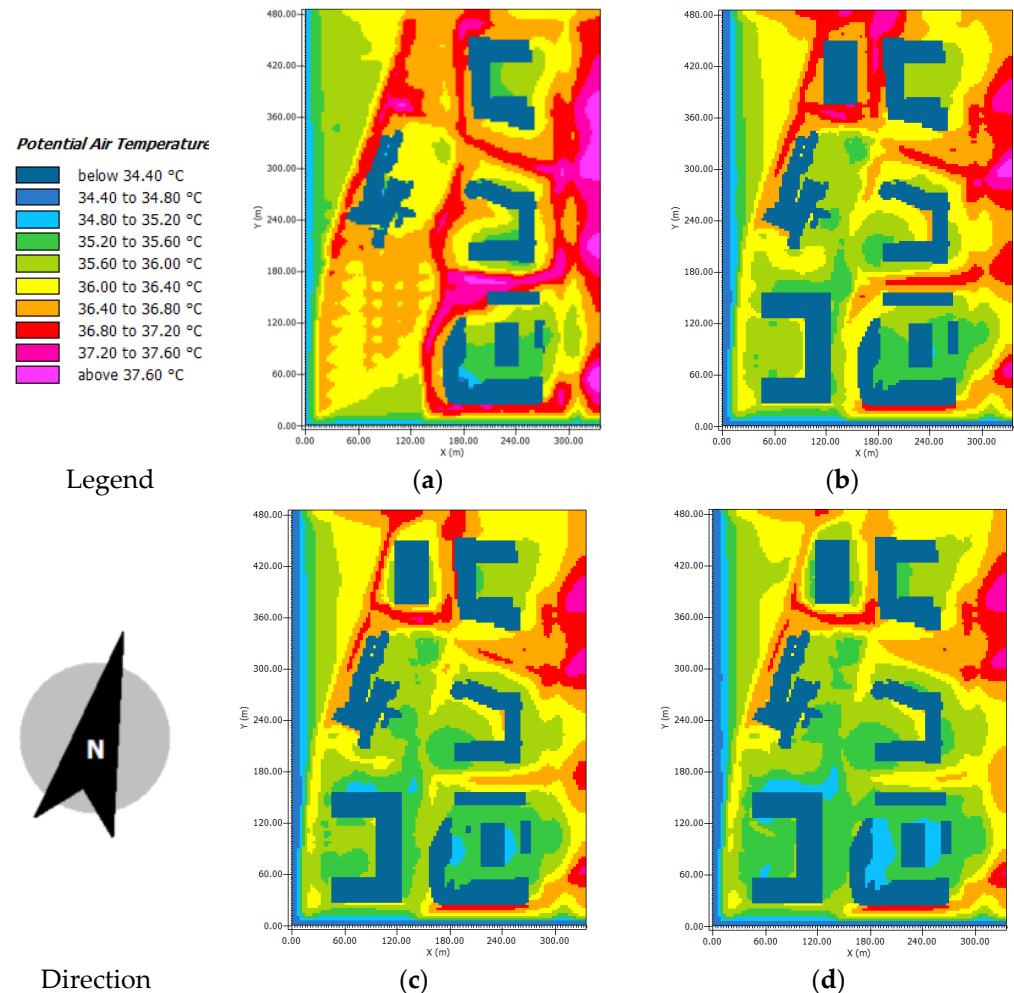


Figure 13. Comparison of simulated T_a obtained at the height of 1.5 m at 15:00 for different H/W. (a) Base case (A0); (b) H/W = 0.8 (A4); (c) H/W = 1 (A5); (d) H/W = 1.2 (A6).

The street on the east side of building four is used as an example. The T_{mrt} of the base cases and the cases with different H/W are shown in Figure 14. As the building height increases, the T_{mrt} of the three cases decreases, and the order is $A6 > A5 > A4$. The highest T_{mrt} difference was recorded at 12:00. The T_{mrt} of A6 was 10.6 °C lower than that of A0. It is concluded that campus streets with a higher H/W have higher outdoor thermal comfort in summer. Case A4 (H/W = 0.8) exhibited the largest difference in the T_{mrt} (the maximum T_{mrt} was 8.7 °C lower than that of A0). The reason is that the streets have buildings on both sides, providing a larger shadow area. However, when the H/W increased from 0.8 to 1 (case A5), the difference in T_{mrt} was relatively small, and when H/W increased from 1 to 1.2 (case A6), there was a negligible difference in T_{mrt} .

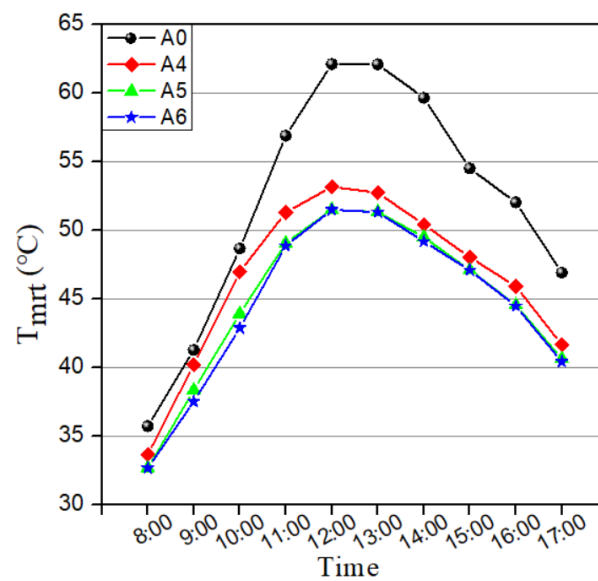


Figure 14. T_{mrt} of the base case and cases with different H/W.

Figure 15 shows the PET for the four cases of 8:00, 12:00, and 15:00. The simulation results show that the PET value of A4 is significantly lower than those of A0, it is 0.2 °C lower at 8:00, 5.1 °C lower at 12:00, and 5.5 °C lower at 15:00. The results demonstrate increasing the building height improves the outdoor thermal environment, and the higher the temperature, the more pronounced the effect is. The PET of case A5 is 1.2 °C lower than that of A4 at 15:00. Increasing the building height increases the H/W, resulting in shorter sun exposure and less solar radiation. However, the difference in the PET between case A6 and case A5 is almost 0, which is consistent with the difference in the T_{mrt} . The likely reason is that as the H/W increase, the influence on the SVF decreases, and the shading effect is less pronounced.

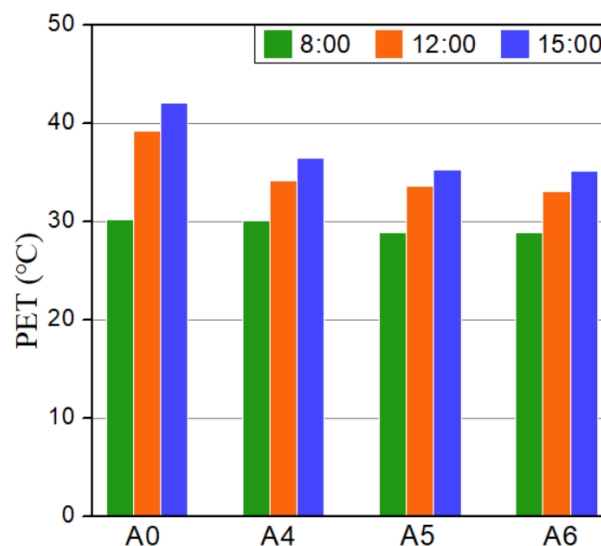


Figure 15. PET of the base case and cases with different H/W at 8:00, 12:00, and 15:00.

3.4. Effect of Surface Albedo

Figure 16 shows the difference in the air temperature between each case and the base case for surfaces with different albedo values. Figure 16a–d indicates that the surface with a high albedo has a low air temperature. The highest cooling effect is achieved for case A10 (1.44 °C). A small difference in the temperature is observed near the asphalt pavement

(0.15–0.45 °C), and the temperature in the other areas is almost unchanged. When the ground albedo is 0.3, the temperature difference ranges from 0 °C to 0.75 °C. The largest cooling effect is observed in the northeast. A large area of asphalt in the east with an albedo of 0.4 also shows a cooling effect. Figure 16e–g shows that increasing the albedo of the masonry has a negligible effect on the temperature of most areas. The temperature difference of the area near the masonry is 0.15 °C to 0.45 °C, and that of a few areas around the building is greater than 1.2 °C. Case A13 exhibits the highest cooling effect, i.e., a maximum difference of 1.4 °C. Overall, increasing the ground albedo results in a slight cooling effect on the hard pavement and surrounding area. The cooling effect is more pronounced at a higher albedo.

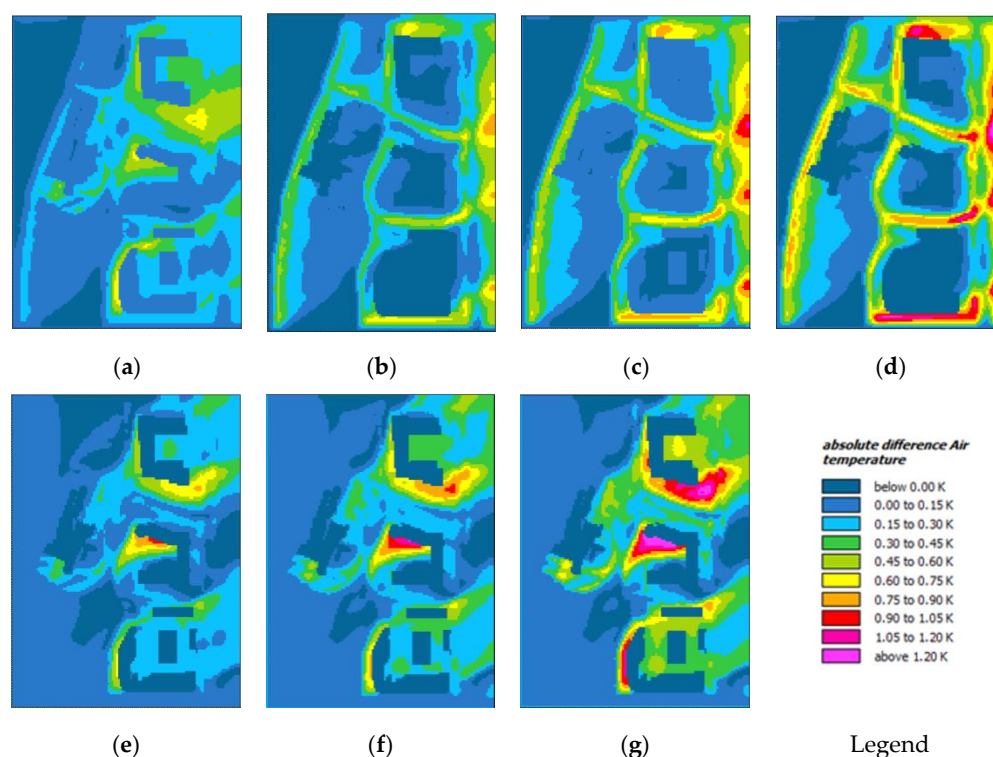


Figure 16. Difference in air temperature between each case and the base case at a height of 1.5 m at 15:00 for surfaces with different albedo values. (a) Asphalt albedo: 0.3 (difference between cases A7 and A0); (b) Asphalt albedo: 0.4 (difference between cases A8 and A0); (c) Asphalt albedo: 0.5 (difference between cases A9 and A0); (d) Asphalt albedo: 0.6 (difference between cases A10 and A0); (e) Masonry albedo: 0.4 (difference between cases A11 and A0); (f) Masonry albedo: 0.5 (difference between cases A12 and A0); (g) Masonry albedo: 0.6 (difference between cases A13 and A0).

Figure 17 shows the T_{mrt} of the base case and the cases with different surface albedo values. The results indicate that the thermal comfort is slightly worse for the cases with higher albedo values. Increasing the surface albedo does not reduce the T_{mrt} but increases it after 9:00. At 12:00, the T_{mrt} of the asphalt with an albedo of 0.6 is 3.7 °C higher than that of A0. The reason is that an increase in the ground albedo increases the shortwave radiation at the location, thereby increasing the total radiation. Similarly, a high surface albedo results in a higher PET, as shown in Figure 18. The effect on the PET is negligible at 8:00, but the PET increases with the albedo at 12:00 and 15:00. The PET of case A10 at 15:00 is 44.99 °C, which is 4.3 °C higher than the PET of A0, significantly reducing the students' thermal comfort. It is concluded that increasing the albedo of the surface reduces the air temperature. However, although the human body benefits from the cool road surface, it is affected by the increase in radiation. The resulting increases in the T_{mrt} and PET cause discomfort to the human body. Therefore, surfaces with a high albedo have variable effects.

Fewer surfaces should be covered with asphalt and concrete, and more areas should be planted with vegetation, such as grass and trees.

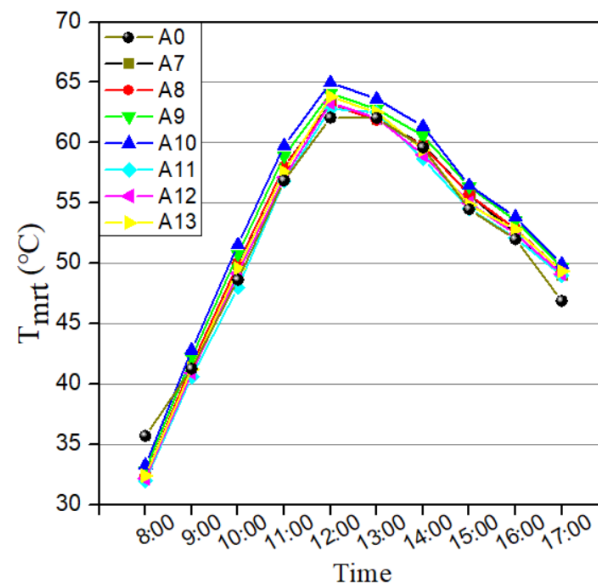


Figure 17. T_{mrt} of the base case and cases with different surface albedo values.

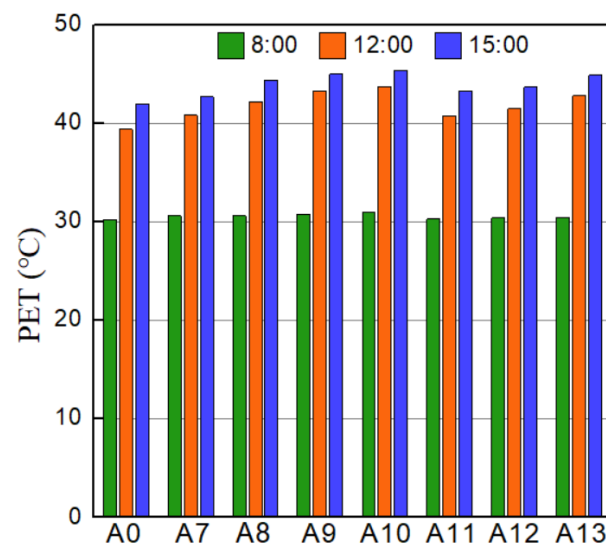


Figure 18. PET of the base case and cases with different surface albedo values at 8:00, 12:00, and 15:00.

4. Discussion

This study focused on three optimization parameters to improve the outdoor thermal comfort of a campus in hot summer weather: vegetation greening, building shading, and surface albedo. The results of the micrometeorological simulations showed that a higher greening rate resulted in a more comfortable outdoor thermal environment on campus. These findings are in line with previous studies support the results here [37,70]. Evergreen trees can reduce thermal comfort in winter by blocking the sunlight. Deciduous trees provide shade in summer and let sunlight reach buildings in winter [71,72]. In addition, according to the results of the field investigation, the deciduous trees with a height of 12 m and a crown width of 9 m were selected in this model. Based on the campus greening characteristics, the central greening in the model is arranged in blocks, and the greening along streets and buildings is arranged in lines. These make our study more reliable.

We investigated the effects of different building heights (H/W). Campus spaces surrounded by buildings with a high H/W have less exposure to solar radiation, resulting in

higher thermal comfort in hot summer. This study showed that a H/W exceeding one did not significantly improve the outdoor thermal environment. Considering the characteristic of cold and severe cold climate zones, students prefer more sunshine in winter. Therefore, the tradeoff between advantages and disadvantages in hot and cold seasons should be considered in the building design to improve outdoor thermal comfort.

The outdoor thermal environment of university campuses can be improved by changing the building facade materials and paving materials. We attempted to improve the outdoor thermal environment by using materials (asphalt and masonry) with a high albedo. Although the surfaces with a high albedo had lower temperatures, the thermal environment near the ground was not improved, which was consistent with the existing findings [48,54]. Therefore, surfaces with a suitable albedo should be selected.

This study has some limitations. First, we used a high greening rate to improve the outdoor thermal environment of the campus. Other greening strategies include various tree planting patterns, different tree species, vertical greening, and other factors. The influence of different greening elements and combinations on the outdoor thermal environment of campuses should be carefully considered.

Moreover, in addition to improving the students' comfort by optimizing meteorological parameters, the students' adaptability is also an important factor. Some studies have found that students' behavior, thermal preferences, and psychological factors affect outdoor thermal sensation [73,74]. Referring to Lam's work, students' perceptions of the outdoor thermal environment were influenced by psychological and physiological factors (such as emotion, fatigue, and region) [75]. Students' thermal sensation was also influenced by seasonal factors. Most students preferred slightly warm conditions in winter and slightly cool conditions in summer [76]. Our research focused on optimizing the design characteristics but did not consider the students' characteristics. Therefore, student behavior, psychology, and physiology should be considered to optimize outdoor thermal comfort.

In summary, future studies will consider landscape design factors, annual climate characteristics, and students' behaviors to provide more insights into optimizing outdoor thermal comfort. The ultimate goal is to create a science-based and efficient outdoor thermal environment optimization strategy to provide reliable information for urban designers and campus planners.

5. Conclusions

This study investigated outdoor thermal comfort in an open space of a campus in a cold region of China. Different optimization strategies (vegetation greening, H/W of buildings, and surface albedo) were analyzed using ENVI-met. The main findings are as follows.

- (1) The field test showed that the temperature of the campus reached 38.4 °C at noon in summer, and the temperature in areas without shade was above 36 °C, adversely affecting the students' outdoor activities. Thermal imagery showed very high surface temperatures of pavement and walls, ranging from 44 °C to 51 °C. In contrast, the surface temperatures in areas shaded by vegetation and buildings were much lower, ranging from 31 °C to 35 °C.
- (2) An increase in the greening rate reduced the air temperature and improved outdoor thermal comfort. This effect became more pronounced as the greening increased from 25% to 45%. At a greening rate of 45%, the maximum T_a , T_{mrt} , and PET were 3.2 °C, 14.4 °C, and 6.9 °C lower, respectively, than in the base case.
- (3) As the H/W of the building increased, the shadow area during the day increased, reducing the SVF. The T_a , T_{mrt} , and PET were 2 °C, 8.7 °C, and 5.5 °C lower, respectively, when there were buildings on both sides of the open area (H/W = 0.8). An increase in the H/W from 0.8 to 1 did not further improve the outdoor thermal comfort. A negligible difference in the T_{mrt} and PET was observed between a H/W of 1 and 1.2. Therefore, increasing the building height improves the thermal environment of the

campus in summer, but a higher building height does not necessarily mean a better thermal environment.

- (4) The air temperature decreased with an increase in the surface albedo. As the albedo increased from 0.2 to 0.6, the maximum temperature dropped by 1.44 °C. However, a decrease in the temperature led to an increase in T_{mrt} and PET, especially in areas in building shadows. The T_{mrt} (PET) of the surface with an albedo of 0.6 was 3.7 °C (4.3 °C) higher than that of the base case. Therefore, the building and ground surfaces should not have a very high albedo.
- (5) Further studies will consider landscape design factors, annual climate characteristics, and students' behaviors to provide more insights into optimizing the outdoor thermal comfort of the university campuses.

Author Contributions: Conceptualization, L.Y. and J.L.; methodology, J.L.; software, L.Y.; validation, L.Y., S.Z. and J.L.; formal analysis, L.Y.; investigation, L.Y., J.L. and S.Z.; resources, J.L.; data curation, L.Y., S.Z. and J.L.; writing—original draft preparation, L.Y., S.Z. and J.L.; writing—review and editing, L.Y., S.Z. and J.L.; visualization, L.Y.; supervision, J.L. and S.Z.; project administration, J.L.; funding acquisition, J.L. All authors have read and agreed to the published version of the manuscript.

Funding: This work was funded by Natural Science Foundation of Shandong Province (ZR2021ME199, ZR2021ME237).

Data Availability Statement: Not applicable.

Acknowledgments: This work acknowledges the Plan of Introduction and Cultivation for Young Innovative Talents in Colleges and Universities of Shandong Province.

Conflicts of Interest: The authors declare no conflict of interest.

Nomenclature

D	globe diameter, mm
G	solar radiation, W/m^2
RH	relative humidity, %
T_a	air temperature, °C
T_g	black globe temperature, °C
T_{mrt}	the mean radiation temperature, °C
V_a	wind speed, m/s
V_{a0}	wind speed at 1.5 m, m/s
V_{a10}	wind speed at 10 m, m/s
z_0	distance from the ground at 1.5 m
z_{10}	distance from the ground at 10 m
Abbreviation	
H/W	height-to-width ratio
PET	physiological equivalent temperature, °C
PMV	predicted mean vote
SVF	sky view factor
UTCI	universal thermal climate index, °C
Greek Symbols	
ε	emissivity
Superscripts	
α	roughness index
Subscripts	
a	air
g	globe
mrt	mean radiation temperature

References

1. Lai, D.; Guo, D.; Hou, Y.; Lin, C.; Chen, Q. Studies of outdoor thermal comfort in northern China. *Build. Environ.* **2014**, *77*, 110–118. [[CrossRef](#)]
2. Xu, M.; Hong, B.; Mi, J.; Yan, S. Outdoor thermal comfort in an urban park during winter in cold regions of China. *Sustain. Cities Soc.* **2018**, *43*, 208–220. [[CrossRef](#)]
3. Zhang, L.; Yu, Z.; Liu, J.; Zhang, L. The numerical analysis of outdoor wind and thermal environment in a residential area in Liaocheng, China. *IOP Conf. Ser. Earth Environ. Sci.* **2018**, *121*, 052054. [[CrossRef](#)]
4. An, F.; Liu, J.; Lu, W.; Jareemit, D. A review of the effect of traffic-related air pollution around schools on student health and its mitigation. *J. Transp. Health* **2021**, *23*, 101249. [[CrossRef](#)]
5. Liu, J.; Cai, W.; Zhu, S.; Dai, F. Impacts of vehicle emission from a major road on spatiotemporal variations of neighborhood particulate pollution—A case study in a university campus. *Sustain. Cities Soc.* **2020**, *53*, 101917. [[CrossRef](#)]
6. Liang, X.; Tian, W.; Li, R.; Niu, Z.; Yang, X.; Meng, X.; Jin, L.; Yan, J. Numerical investigations on outdoor thermal comfort for built environment: Case study of a Northwest campus in China. *Energy Procedia* **2019**, *158*, 6557–6563. [[CrossRef](#)]
7. Zhang, L.; Zhang, L.; Jin, M.; Liu, J. Numerical Study of Outdoor Thermal Environment in a University Campus in Summer. *Procedia Eng.* **2017**, *205*, 4052–4059. [[CrossRef](#)]
8. Lam, C.K.C.; Weng, J.; Liu, K.; Hang, J. The effects of shading devices on outdoor thermal and visual comfort in Southern China during summer. *Build. Environ.* **2022**, *228*, 109743. [[CrossRef](#)]
9. Zhao, T.F.; Fong, K.F. Characterization of different heat mitigation strategies in landscape to fight against heat island and improve thermal comfort in hot-humid climate (Part I): Measurement and modelling. *Sustain. Cities Soc.* **2017**, *32*, 523–531. [[CrossRef](#)]
10. Ghaffarianhoseini, A.; Berardi, U.; Ghaffarianhoseini, A.; Al-Obaidi, K. Analyzing the thermal comfort conditions of outdoor spaces in a university campus in Kuala Lumpur, Malaysia. *Sci. Total Environ.* **2019**, *666*, 1327–1345. [[CrossRef](#)]
11. Berardi, U. The outdoor microclimate benefits and energy saving resulting from green roofs retrofits. *Energy Build.* **2016**, *121*, 217–229. [[CrossRef](#)]
12. Abdallah, A.S.H.; Hussein, S.W.; Nayel, M. The impact of outdoor shading strategies on student thermal comfort in open spaces between education building. *Sustain. Cities Soc.* **2020**, *58*, 102124. [[CrossRef](#)]
13. Eslamirad, N.; Sepúlveda, A.; De Luca, F.; Sakari Lylykangas, K. Evaluating Outdoor Thermal Comfort Using a Mixed-Method to Improve the Environmental Quality of a University Campus. *Energies* **2022**, *15*, 1577. [[CrossRef](#)]
14. Sun, B.; Zhang, H.; Zhao, L.; Qu, K.; Liu, W.; Zhuang, Z.; Ye, H. Microclimate Optimization of School Campus Landscape Based on Comfort Assessment. *Buildings* **2022**, *12*, 1375. [[CrossRef](#)]
15. Yola, L.; Adekunle, T.O.; Ayegbusi, O.G. The Impacts of Urban Configurations on Outdoor Thermal Perceptions: Case Studies of Flat Bandar Tasik Selatan and Surya Magna in Kuala Lumpur. *Buildings* **2022**, *12*, 1684. [[CrossRef](#)]
16. Liu, L.; Liang, Z.; Liu, J.; Du, J.; Zhang, H. Field Survey on Local Thermal Comfort of Students at a University Campus: A Case Study in Shanghai. *Atmosphere* **2022**, *13*, 1433. [[CrossRef](#)]
17. Huang, T.; Li, J.; Xie, Y.; Niu, J.; Mak, C.M. Simultaneous environmental parameter monitoring and human subject survey regarding outdoor thermal comfort and its modelling. *Build. Environ.* **2017**, *125*, 502–514. [[CrossRef](#)]
18. Lai, D.; Zhou, X.; Chen, Q. Modelling dynamic thermal sensation of human subjects in outdoor environments. *Energy Build.* **2017**, *149*, 16–25. [[CrossRef](#)]
19. Zhao, L.; Zhou, X.; Li, L.; He, S.; Chen, R. Study on outdoor thermal comfort on a campus in a subtropical urban area in summer. *Sustain. Cities Soc.* **2016**, *22*, 164–170. [[CrossRef](#)]
20. Altunkasa, C.; Uslu, C. Use of outdoor microclimate simulation maps for a planting design to improve thermal comfort. *Sustain. Cities Soc.* **2020**, *57*, 102137. [[CrossRef](#)]
21. Khalili, S.; Fayaz, R.; Zolfaghari, S.A. Analyzing outdoor thermal comfort conditions in a university campus in hot-arid climate: A case study in Birjand, Iran. *Urban Clim.* **2022**, *43*, 101128. [[CrossRef](#)]
22. Aghamohammadi, N.; Fong, C.S.; Mohd Idrus, M.H.; Ramakreshnan, L.; Haque, U. Outdoor thermal comfort and somatic symptoms among students in a tropical city. *Sustain. Cities Soc.* **2021**, *72*, 103015. [[CrossRef](#)]
23. He, X.; An, L.; Hong, B.; Huang, B.; Cui, X. Cross-cultural differences in thermal comfort in campus open spaces: A longitudinal field survey in China's cold region. *Build. Environ.* **2020**, *172*, 106739. [[CrossRef](#)]
24. Kumar, P.; Sharma, A. Study on importance, procedure, and scope of outdoor thermal comfort—A review. *Sustain. Cities Soc.* **2020**, *61*, 102297. [[CrossRef](#)]
25. Cheng, V.; Ng, E.; Chan, C.; Givoni, B. Outdoor thermal comfort study in a sub-tropical climate: A longitudinal study based in Hong Kong. *Int. J. Biometeorol.* **2012**, *56*, 43–56. [[CrossRef](#)] [[PubMed](#)]
26. Nie, T.; Lai, D.; Liu, K.; Lian, Z.; Yuan, Y.; Sun, L. Discussion on inapplicability of Universal Thermal Climate Index (UTCI) for outdoor thermal comfort in cold region. *Urban Clim.* **2022**, *46*, 101304. [[CrossRef](#)]
27. Deng, J.-Y.; Wong, N.H.; Zheng, X. Effects of street geometries on building cooling demand in Nanjing, China. *Renew. Sustain. Energy Rev.* **2021**, *142*, 110862. [[CrossRef](#)]
28. Li, J.; Liu, J.; Srebric, J.; Hu, Y.; Liu, M.; Su, L.; Wang, S. The Effect of Tree-Planting Patterns on the Microclimate within a Courtyard. *Sustainability* **2019**, *11*, 1665. [[CrossRef](#)]
29. Kleerekoper, L.; Van Esch, M.; Salcedo, T.B. How to make a city climate-proof, addressing the urban heat island effect. *Resour. Conserv. Recycl.* **2012**, *64*, 30–38. [[CrossRef](#)]

30. Teshnehdel, S.; Akbari, H.; Di Giuseppe, E.; Brown, R.D. Effect of tree cover and tree species on microclimate and pedestrian comfort in a residential district in Iran. *Build. Environ.* **2020**, *178*, 106899. [\[CrossRef\]](#)
31. Xu, C.; Yan, C.; Ren, J.; Liu, J. Numerical analysis the effect of trees on the outdoor thermal environment and the building energy consumption in a residential neighborhood. *IOP Conf. Ser. Earth Environ. Sci.* **2020**, *546*, 032007.
32. Jin, M.; Liu, J.; Zhang, L. Numerical Evaluation of the Impact of Green Wall on the Outdoor Thermal Environment. In Proceedings of the 2016 3rd International Conference on Materials Engineering, Manufacturing Technology and Control, Taiyuan, China, 27–28 February 2016.
33. Aflaki, A.; Mirnezhad, M.; Ghaffarianhoseini, A.; Ghaffarianhoseini, A.; Omrany, H.; Wang, Z.-H.; Akbari, H. Urban heat island mitigation strategies: A state-of-the-art review on Kuala Lumpur, Singapore and Hong Kong. *Cities* **2017**, *62*, 131–145. [\[CrossRef\]](#)
34. Wang, Y.; Akbari, H. The effects of street tree planting on Urban Heat Island mitigation in Montreal. *Sustain. Cities Soc.* **2016**, *27*, 122–128. [\[CrossRef\]](#)
35. Abdi, B.; Hami, A.; Zarehaghi, D. Impact of small-scale tree planting patterns on outdoor cooling and thermal comfort. *Sustain. Cities Soc.* **2020**, *56*, 102085. [\[CrossRef\]](#)
36. Gachkar, D.; Taghvaei, S.H.; Norouzian-Maleki, S. Outdoor thermal comfort enhancement using various vegetation species and materials (case study: Delgosha Garden, Iran). *Sustain. Cities Soc.* **2021**, *75*, 103309. [\[CrossRef\]](#)
37. Yang, Y.; Zhou, D.; Wang, Y.; Ma, D.; Chen, W.; Xu, D.; Zhu, Z. Economical and outdoor thermal comfort analysis of greening in multistory residential areas in Xi'an. *Sustain. Cities Soc.* **2019**, *51*, 101730. [\[CrossRef\]](#)
38. Liu, J.; Heidarinejad, M.; Pitchurov, G.; Zhang, L.; Srebric, J. An extensive comparison of modified zero-equation, standard k- ϵ , and LES models in predicting urban airflow. *Sustain. Cities Soc.* **2018**, *40*, 28–43. [\[CrossRef\]](#)
39. Liu, J.; Heidarinejad, M.; Gracik, S.; Srebric, J. The impact of exterior surface convective heat transfer coefficients on the building energy consumption in urban neighborhoods with different plan area densities. *Energy Build.* **2015**, *86*, 449–463. [\[CrossRef\]](#)
40. Xiong, K.; He, B.-J. Wintertime outdoor thermal sensations and comfort in cold-humid environments of Chongqing China. *Sustain. Cities Soc.* **2022**, *87*, 104203. [\[CrossRef\]](#)
41. Hang, J.; Wang, D.; Zeng, L.; Ren, L.; Shi, Y.; Zhang, X. Scaled outdoor experimental investigation of thermal environment and surface energy balance in deep and shallow street canyons under various sky conditions. *Build. Environ.* **2022**, *225*, 109618. [\[CrossRef\]](#)
42. Mahmoud, H.; Ghanem, H.; Sodoudi, S. Urban geometry as an adaptation strategy to improve the outdoor thermal performance in hot arid regions: Aswan University as a case study. *Sustain. Cities Soc.* **2021**, *71*, 102965. [\[CrossRef\]](#)
43. Kakon, A.N.; Mishima, N.; Kojima, S. Simulation of the urban thermal comfort in a high density tropical city: Analysis of the proposed urban construction rules for Dhaka, Bangladesh. *Build. Simul.* **2009**, *2*, 291–305. [\[CrossRef\]](#)
44. Wu, J.; Chang, H.; Yoon, S. Numerical Study on Microclimate and Outdoor Thermal Comfort of Street Canyon Typology in Extremely Hot Weather—A Case Study of Busan, South Korea. *Atmosphere* **2022**, *13*, 307. [\[CrossRef\]](#)
45. Qaid, A.; Bin Lamit, H.; Ossen, D.R.; Shahminan, R.N.R. Urban Heat Island and Thermal Comfort Conditions at Micro-climate Scale in a Tropical Planned City. *Energy Build.* **2016**, *133*, 577–595. [\[CrossRef\]](#)
46. Charalampopoulos, I.; Tsiros, I.; Chronopoulou-Sereli, A.; Matzarakis, A. Analysis of thermal bioclimate in various urban configurations in Athens, Greece. *Urban Ecosyst.* **2013**, *16*, 217–233. [\[CrossRef\]](#)
47. Wang, S.; Chen, B.; Suo, J.; Zhao, J.R. Impact of building morphology and outdoor environment on light and thermal environment in campus buildings in cold region during winter. *Build. Environ.* **2021**, *204*, 108074. [\[CrossRef\]](#)
48. Taleghani, M.; Berardi, U. The effect of pavement characteristics on pedestrians' thermal comfort in Toronto. *Urban Clim.* **2018**, *24*, 449–459. [\[CrossRef\]](#)
49. Del Serrone, G.; Peluso, P.; Moretti, L. Evaluation of Microclimate Benefits Due to Cool Pavements and Green Infrastructures on Urban Heat Islands. *Atmosphere* **2022**, *13*, 1586. [\[CrossRef\]](#)
50. Liu, J.; Heidarinejad, M.; Nikkho, S.K.; Mattise, N.W.; Srebric, J. Quantifying Impacts of Urban Microclimate on a Building Energy Consumption—A Case Study. *Sustainability* **2019**, *11*, 4921. [\[CrossRef\]](#)
51. Heidarinejad, M.; Gracik, S.; Sadeghipour Roudsari, M.; Khoshdel Nikkho, S.; Liu, J.; Liu, K.; Pitchurov, G.; Srebric, J. Influence of building surface solar irradiance on environmental temperatures in urban neighborhoods. *Sustain. Cities Soc.* **2016**, *26*, 186–202. [\[CrossRef\]](#)
52. Hendel, M. Chapter 11: 6—Cool pavements. In *Eco-Efficient Pavement Construction Materials*; Pacheco-Torgal, F., Amirkhanian, S., Wang, H., Schlangen, E., Eds.; Woodhead Publishing: Sawston/Cambridge, UK, 2020; pp. 97–125.
53. Pisello, A.L.; Cotana, F. The thermal effect of an innovative cool roof on residential buildings in Italy: Results from two years of continuous monitoring. *Energy Build.* **2014**, *69*, 154–164. [\[CrossRef\]](#)
54. Rosso, F.; Pisello, A.L.; Cotana, F.; Ferrero, M. On the thermal and visual pedestrians' perception about cool natural stones for urban paving: A field survey in summer conditions. *Build. Environ.* **2016**, *107*, 198–214. [\[CrossRef\]](#)
55. Castaldo, V.L.; Coccia, V.; Cotana, F.; Pignatta, G.; Pisello, A.L.; Rossi, F. Thermal-energy analysis of natural "cool" stone aggregates as passive cooling and global warming mitigation technique. *Urban Clim.* **2015**, *14*, 301–314. [\[CrossRef\]](#)
56. Salata, F.; Golasi, I.; Petitti, D.; De Lieto Vollaro, E.; Coppi, M.; De Lieto Vollaro, A. Relating microclimate, human thermal comfort and health during heat waves: An analysis of heat island mitigation strategies through a case study in an urban outdoor environment. *Sustain. Cities Soc.* **2017**, *30*, 79–96. [\[CrossRef\]](#)

57. Yang, J.; Wang, Z.-H.; Kaloush, K.E.; Dylla, H. Effect of pavement thermal properties on mitigating urban heat islands: A multi-scale modeling case study in Phoenix. *Build. Environ.* **2016**, *108*, 110–121. [[CrossRef](#)]
58. Meteoblue Weather. Available online: https://www.meteoblue.com/en/weather/historyclimate/climatemodelled/tianzhuangcun_china_12341129 (accessed on 23 November 2022).
59. Jendritzky, G.; Nübler, W. A model analysing the urban thermal environment in physiologically significant terms. *Arch. Meteorol. Geophys. Bioclimatol. Ser. B* **1981**, *29*, 313–326. [[CrossRef](#)]
60. Frank, R.S.; Gerding, R.B.; O’rourke, P.A.; Terjung, W.H. An urban radiation obstruction model. *Bound. -Layer Meteorol.* **1981**, *20*, 259–264. [[CrossRef](#)]
61. Salata, F.; Golasi, I.; De Lieto Vollaro, R.; De Lieto Vollaro, A. Urban microclimate and outdoor thermal comfort. A proper procedure to fit ENVI-met simulation outputs to experimental data. *Sustain. Cities Soc.* **2016**, *26*, 318–343. [[CrossRef](#)]
62. Matzarakis, A.; Rutz, F.; Mayer, H. Modelling radiation fluxes in simple and complex environments: Basics of the RayMan model. *Int. J. Biometeorol.* **2010**, *54*, 131–139. [[CrossRef](#)]
63. Matzarakis, A.; Rutz, F.; Mayer, H. Modelling radiation fluxes in simple and complex environments—Application of the RayMan model. *Int. J. Biometeorol.* **2007**, *51*, 323–334. [[CrossRef](#)]
64. Ali-Thoudert, F.; Mayer, H. Numerical study on the effects of aspect ratio and orientation of an urban street canyon on outdoor thermal comfort in hot and dry climate. *Build. Environ.* **2006**, *41*, 94–108. [[CrossRef](#)]
65. Emmanuel, R.; Rosenlund, H.; Johansson, E. Urban shading—A design option for the tropics? A study in Colombo, Sri Lanka. *Int. J. Climatol.* **2010**, *27*, 1995–2004. [[CrossRef](#)]
66. Morakinyo, T.E.; Dahanayake, K.W.D.K.C.; Adegun, O.B.; Balogun, A.A. Modelling the effect of tree-shading on summer indoor and outdoor thermal condition of two similar buildings in a Nigerian university. *Energy Build.* **2016**, *130*, 721–732. [[CrossRef](#)]
67. Middel, A.; Chhetri, N.; Quay, R. Urban forestry and cool roofs: Assessment of heat mitigation strategies in Phoenix residential neighborhoods. *Urban For. Urban Green.* **2015**, *14*, 178–186. [[CrossRef](#)]
68. Taleghani, M. The impact of increasing urban surface albedo on outdoor summer thermal comfort within a university campus. *Urban Clim.* **2018**, *24*, 175–184. [[CrossRef](#)]
69. Oke, T.R. Street design and urban canopy layer climate. *Energy Build.* **1988**, *11*, 103–113. [[CrossRef](#)]
70. Lee, H.; Mayer, H. Maximum extent of human heat stress reduction on building areas due to urban greening. *Urban For. Urban Green.* **2018**, *32*, 154–167. [[CrossRef](#)]
71. Lin, T.-P.; Tsai, K.-T.; Hwang, R.-L.; Matzarakis, A. Quantification of the effect of thermal indices and sky view factor on park attendance. *Landsc. Urban Plann.* **2012**, *107*, 137–146. [[CrossRef](#)]
72. El-Bardisy, W.M.; Fahmy, M.; El-Gohary, G.F. Climatic Sensitive Landscape Design: Towards a Better Microclimate through Plantation in Public Schools, Cairo, Egypt. *Procedia Soc. Behav. Sci.* **2016**, *216*, 206–216. [[CrossRef](#)]
73. Vanos, J.K.; Warland, J.S.; Gillespie, T.J.; Kenny, N.A. Review of the physiology of human thermal comfort while exercising in urban landscapes and implications for bioclimatic design. *Int. J. Biometeorol.* **2010**, *54*, 319–334. [[CrossRef](#)]
74. Lin, T.-P. Thermal perception, adaptation and attendance in a public square in hot and humid regions. *Build. Environ.* **2009**, *44*, 2017–2026. [[CrossRef](#)]
75. Lam, C.K.C.; Hang, J.; Zhang, D.; Wang, Q.; Ren, M.; Huang, C. Effects of short-term physiological and psychological adaptation on summer thermal comfort of outdoor exercising people in China. *Build. Environ.* **2021**, *198*, 107877. [[CrossRef](#)]
76. Huang, Z.; Cheng, B.; Gou, Z.; Zhang, F. Outdoor thermal comfort and adaptive behaviors in a university campus in China’s hot summer-cold winter climate region. *Build. Environ.* **2019**, *165*, 106414. [[CrossRef](#)]